Measurement of interfacial structure for co-current air–water flow

By LEMBIT U. LILLELEHT† AND THOMAS J. HANRATTY

Department of Chemistry and Chemical Engineering, University of Illinois, Urbana, Illinois

(Received 19 January 1961)

A method for measuring the interfacial structure between a co-current air–water flow using the absorption of light is described. Measurements of the root-mean-squared displacement and the frequency spectrum are presented. The use of a Gaussian model to describe the interface is explored.

1. Introduction

An understanding of the interaction between an air stream and a flowing liquid film is important to many engineering processes. A rectangular channel having an aspect ratio of 12 to 1 has been used in this laboratory to study the interaction. The liquid is injected through the bottom of the channel, and the air flows co-currently over the liquid surface. If a long enough channel is used, a fully developed condition is attained downstream in which there is no further change in the flow condition of the gas or the liquid. Pressure taps in the top of the channel allow measurement of the pressure gradient, which is the same in both the gas and the liquid. A total-head tube entering through the top wall is used to measure the velocity profile in the gas. The average shear stress at the interface between the air and the liquid can be calculated from the location of the maximum in the gas velocity and the pressure gradient.

Five types of interfacial structures have been described by Hanratty & Engen (1957) for air–water flow. For a fixed flow rate of the liquid, the following sequence of flow régimes is noted as the gas flow is increased: (1) smooth, (2) two-dimensional waves, (3) three-dimensional waves, (4) roll-waves, and (5) dispersed flow. At low enough gas flows no waves are visible to the eye, even though the air flow might be turbulent. The first disturbance which appears on the surface as the gas flow increases are low-amplitude two-dimensional waves extending over the whole width of the channel. They are nearly 0·4 in. apart and travel with a velocity of 0·75 to 1 ft./sec. If the gas velocity is increased only slightly above the transition condition for two-dimensional waves, a pebbled three-dimensional wave structure appears. The wavelength is 0·2–0·4 in. and the wave breadth is approximately equal to the length. The three-dimensional wave structure is stable over a wide range of gas flows. Eventually, however, roll waves appear at the interface. These are two-dimensional disturbances of large

† Now at the University of Alberta, Edmonton, Alberta, Canada.

wavelength with a steep front and long sloping back, which move over the three-dimensional structure and which resemble waves rolling in on a beach. At sufficiently high flow rates, droplets are torn from the liquid surface and the liquid becomes dispersed in the gas phase.

The transitions to these different flow régimes has been studied using a highly disturbed liquid entry (Hanratty & Engen 1957; Hershman 1960; Oosterhout 1958), and a theory explaining the roll-wave transition has been developed by Hanratty & Hershman (1960). The wave structures at the interface cause an increase in the interfacial shear stress over what would exist for a smooth surface in much the same way as roughness elements on solid surfaces (cf. Ellis 1959; Ellison 1956; Hanratty & Engen 1957; van Rossum 1959). The description of the liquid interfacial structure in the papers mentioned above has been based on visual observations. An understanding of the relation of the interfacial structure and of the increase of interfacial stress to system variables depends on a more exact definition of the waves. A technique for measuring the instantaneous height of the liquid has been developed for this purpose (Lilleleht 1961). The present paper has been written to describe the technique and to present the results of some of the initial measurements of the interfacial structure. The relation of interfacial structure to the interfacial shear stress is described in another paper (Lilleleht & Hanratty 1960).

A fine beam of light is passed through the top of the channel and the liquid film and is impinged on a photomultiplier tube. If methylene-blue dye is dissolved in the liquid, a large portion of the light will be absorbed by the liquid, and variations in the height of the liquid film will cause variations in the output signal from the photomultiplier tube. During the period of the development of the above technique in this laboratory, we became aware of similar work which had been done at the Purdue University Jet Propulsion Center by Greenberg (1956) and Charvonia (1959). However, although the basic techniques are the same, there are sufficient differences in the design of the experiments to justify the detailed description of the measurements given in this paper.

The numerical techniques used in this paper to characterize the wave structure are the same as those that have been used for the surface of large bodies of water (Hicks & Whittenbury 1956; Pierson 1955; Putz 1954). The height of the liquid film is defined as the sum of an average height and a fluctuating component. The fluctuating component is described in terms of the variance, the distribution functions describing liquid height and crest height, the frequency spectrum, and the number of crossings at a fixed height. Average film heights for horizontal air–liquid flows have been determined by Hershman (1960) and by van Rossum (1959) using conductance measurements, and by McManus (1959) using an electrical contacting method with a gauge connected to a micrometer screw Average height measurements have been made by Greenberg (1956) and by Charvonia (1959) using a photoelectric method for the co-current flow of air and water inside a vertical pipe. Charvonia has also presented measurements of wave-height distributions for his vertical flow system, and McManus has determined maximum wave heights for air–water flow inside a horizontal pipe.

2. Theory

If the instantaneous height of the liquid film is designated by h then a time average height $\bar{h}$ may be defined as

$$\bar{h} = \lim_{T\to\infty} \frac{1}{T}\int_0^T h\,dt, \tag{2.1}$$

and a fluctuating height h' may be defined by

$$h = \bar{h} + h'. \tag{2.2}$$

The variance of the height, designated by $\Delta(h')$, is the root-mean-squared value of h': thus

$$\Delta(h') = (\overline{h'^2})^{\frac{1}{2}} = \left[\lim_{T\to\infty} \frac{1}{T}\int_0^T h'^2 dT\right]^{\frac{1}{2}}. \tag{2.3}$$

A probability function may be defined by

$$P(h)\,dh = \text{fraction of the time the film height has a value between } h \text{ and } h+dh; \tag{2.4}$$

and if this probability function is Gaussian, we have

$$P(h) = \left(\frac{1}{2\pi}\right)^{\frac{1}{2}} \frac{1}{\Delta(h')} \exp\left\{-\frac{(h-\bar{h})^2}{2[\Delta(h')]^2}\right\}. \tag{2.5}$$

Measurements by Putz (1954) on a large body of water are described quite well by (2.5).

The average number $N(h)$ of times that the function describing h crosses a given value of h in a long period of time is a conveniently measured property, and can be related to the wave structure of the interface. If a wave crest is a maximum and a wave trough is a minimum in h, then $N(h)$ equals twice the difference of the number of crests from the number of troughs at heights greater than h. The difference of $N(h)$ at two values of h is related to the number of maxima and minima in that interval by

$$\tfrac{1}{2}\{N(h_2) - N(h_1)\} = \text{the average number of maxima minus the number of minima in the height interval } h_2 - h_1. \tag{2.6}$$

The above function was measured by Charvonia (1959) in his experiments on air–water flow in a vertical pipe. If, according to Pierson (1955), a wave is defined as the complete cycle during which h passes from $\bar{h}$ up to a crest, then falls through $\bar{h}$ down to a trough and finally passes up through $\bar{h}$ again, then the number of waves per second equals $\frac{1}{2}N(\bar{h})$.

As has been shown by Rice (1944, 1945), a frequency spectrum for the fluctuating height h' can be described as follows:

$$w(f)\,df = \text{fraction of } \overline{h'^2} \text{ contributed by frequencies between } f \text{ and } f+df, \tag{2.7}$$

$$\overline{h'^2} = \int_0^\infty w(f)\,df. \tag{2.8}$$

The frequency spectrum is defined in terms of the Fourier transform of the curve representing h' by the following equations:

$$w(f) = \lim_{T\to\infty} \frac{2\,|S(f)|^2}{T}, \tag{2.9}$$

$$S(f) = \int_0^T h(t)\, e^{-i2\pi ft} dt. \tag{2.10}$$

For cases in which both h' and dh'/dt are normally distributed and are statistically independent, $N(h)$ may be related to the frequency spectrum. Rice gave the results

$$N(\bar{h}) = 2\left[\int_0^\infty f^2 w(f)\, df \Big/ \int_0^\infty w(f)\, df\right]^{\frac{1}{2}}, \tag{2.11}$$

$$N(h) = \exp\left[-(h-\bar{h})^2/2\overline{h'^2}\right] \tfrac{1}{2} N(\bar{h}), \tag{2.12}$$

on the condition that the integrals converge. The expected number of maxima per second is

$$N(h_m) = \left[\int_0^\infty f^4 w(f)\, df \Big/ \int_0^\infty f^2 w(f)\, df\right]^{\frac{1}{2}}. \tag{2.13}$$

Rice also has calculated, on the basis of the Gaussian model, the fraction of the crests with heights greater than h. This result is presented in figure 4 of his paper.

The wave structure under different flow conditions are compared in this paper by means of the functions $w(f)$ and $\Delta(h')$. It will be assumed that the effect of the gas flow over the liquid surface can be described solely by the friction velocity u^*. For the cases considered in this paper, average velocity in a given liquid is fixed for fixed values of u^* and $\bar{h}$. Therefore,

$$\Delta(h') = F(h, u^*, g, \sigma/\rho, \rho, \mu/\rho), \tag{2.14}$$

where σ is the interfacial tension, μ is the liquid viscosity, ρ is the liquid density and g is the acceleration of gravity. If σ/ρ, μ/ρ and ρ are unimportant in so far as they directly affect $\Delta(h')$, then

$$\frac{g\Delta(h')}{u^{*2}} = F\left(\frac{g\bar{h}}{u^{*2}}\right). \tag{2.15}$$

For very deep bodies of water, $\Delta h'$ is independent of $\bar{h}$, and we have

$$\frac{g\Delta(h')}{u^{*2}} = \text{const.} \tag{2.16}$$

Analogous to (2.14), the following expression can be written for the frequency spectrum:

$$w = F(f, h, u^*, g, \sigma/\rho, \rho, \mu/\rho). \tag{2.17}$$

If σ/ρ, μ/ρ, and ρ are unimportant, then

$$\frac{wg^3}{u^{*5}} = F\left[\left(\frac{fu^*}{g}\right), \left(\frac{g\bar{h}}{u^{*2}}\right)\right]. \tag{2.18}$$

By using arguments similar to those used to explain the form of the energy spectrum obtained in turbulence measurements, Phillips (1958) has suggested that

w should be independent of u^* at large frequencies. If for the flows considered it is also independent of $\bar{h}$, then

$$\frac{wf^5}{g^2} = \text{const.} \tag{2.19}$$

Phillips showed that the high-frequency end of the spectrum measured in a reservoir could be represented by the equation

$$\frac{wf^5}{g^2} = 9{\cdot}5 \times 10^{-6}. \tag{2.20}$$

3. Flow system

The design of the flow system used in the experiments described in this paper is similar to that used by Hanratty & Engen (1957) and by Hershman (1960). The 'Plexiglass' channel was 1·020 in. high, 12 in. wide and 21 ft. long. The entry was quite different from that used in previous work in this laboratory. The air and the liquid were brought together at the inlet of the Plexiglass channel. The liquid was introduced into the channel from an entry box fastened to the channel bottom through 60 holes of 0·1540 in. diameter, which were slanted 45° in the direction of liquid flow and which were spaced in a scattered fashion. The liquid-entry area containing the holes was covered with a 6×12 in. piece of 200-mesh copper screen to prevent any possible jetting effects at high rates of liquid flow. This design gave a much smoother entry condition of the liquid film than the one used by Hanratty & Engen. The liquid discharging from the channel was collected in a reservoir and recirculated. Liquid-height measurements were made at a position 11 ft. 8 in. from the channel inlet. A $2\frac{5}{16}$ in. diameter hole was cut in the bottom of the channel at this position and a $\frac{1}{4}$ in. thick circular disk of Plexiglass was inserted into the hole. The top of the channel at the test section consisted of a $3\frac{1}{2}$ in. piece of Plexiglass that could be slid into place. Both the top and bottom pieces at the test section were easily removable to facilitate cleaning, and replacement if they became scratched. The top could also be replaced by the total-head tube assembly for gas phase velocity-profile measurements. Pressure taps on the top of the channel were located 6 ft. 2 in., 12 ft. 8 in. and 15 ft. 2 in. from the entry. A total-head tube mounted on a micrometer screw at a distance 15 ft. 2 in. was used in conjunction with a static pressure tap on the top of the channel to measure the velocity distribution in the air stream. All pressures were measured with a Wahlen manometer (Engen 1956).

4. Measurement of liquid heights

The equipment used to measure the average and instantaneous liquid height is sketched in figure 1. A chopped beam of light is passed through a filter and a lens system, and is focused at the interface between the gas and the liquid as a beam about 1 mm in diameter. It passed through the water containing methylene-blue dye and through the bottom of the channel on to a diffuser screen. The light beam on the diffuser screen was picked up by a photomultiplier tube. The signal from the photomultiplier tube was amplified, clipped, and demodulated to give an electrical signal corresponding to the wave-form.

The light source was chopped in order to eliminate the effect of background light and to simplify the problem of amplifying the signal from the photomultiplier tube. This signal consisted of a DC portion, which was a measure of the background light, and an AC portion whose amplitude varied with the height of the liquid in the channel. By using an AC amplifier, only the AC portion was transmitted to the recording device. A mechanical chopper was used consisting of an aluminium disk with forty $\frac{5}{16}$ in. holes drilled on a 4 in. circle. Each revolution

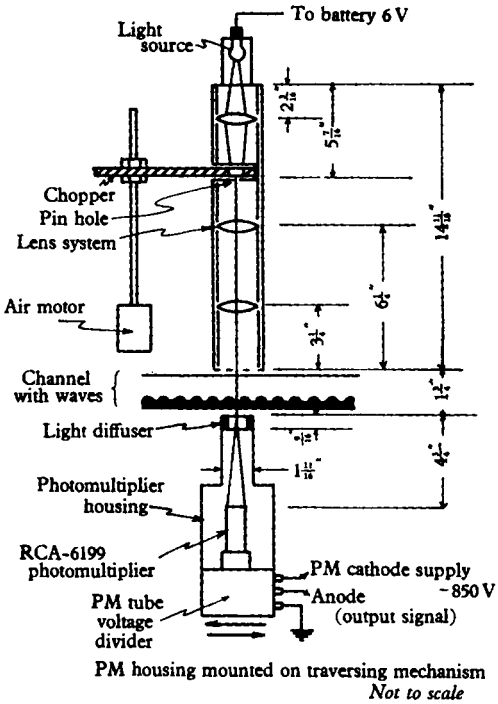

FIGURE 1. Diagram of the lens and photomultiplier arrangement.

of the chopper produced forty rectangular pulses of light. In order to minimize 60-cyc. AC pick-up, the disk was driven by an air motor at a speed of about 40 rev./sec. This produced a light beam of 1600 pulses/sec, or 100 pulses for each cycle of a 16 c/s sine wave. The lens system for focusing the light beam was mounted in a $2\frac{3}{4}$ in. brass tube, plastic spacers being used to locate them in the proper position. The inside of the assembly was painted with a matt black paint to prevent internal reflexions. Several filters were placed in the brass tube to provide a beam approximately 530 mμ in wavelength, such as is strongly absorbed by methylene blue.

An RCA type 6199 photomultiplier tube housed in a $3\frac{1}{2}$ in. cylindrical brass tube was used. It had a 1·24 in. diameter flat face with semi-transparent cathode. In testing the tube it was found that the photocathode was not of uniform sensitivity. Owing to refraction at the liquid–gas interface, the light beam emerged from the gas–liquid interface at different angles from the vertical and, therefore, was aimed at different positions on the cathode surface. Consequently, the non-

uniformity of the photocathode could lead to serious error. A diffuser disk was placed between the bottom of the channel and the photomultiplier tube to diffuse the light uniformly in all directions. The photomultiplier tube was placed approximately 5 in. from the diffuser, so that small movements of the light spot on the diffuser would not affect the solid angle intercepted by the photomultiplier tube. A Beckman 'heliopot' precision potentiometer was used as a load resistor for the photomultiplier tube to take varying fractions of the total output signal for amplification and analysis. The anode was at ground potential and the cathode

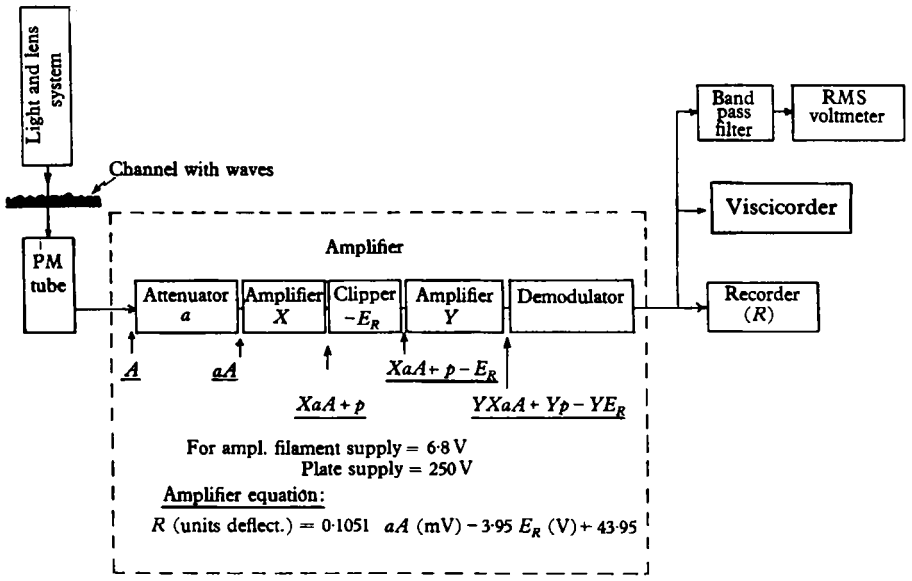

FIGURE 2. Block diagram of electronic equipment.

was at -850 V. Electrostatic shielding of the photomultiplier tube was provided by a closely fitted copper foil covering the uncoated area of the tube and connected through a 12 MΩ resistor to the cathode supply.

A block diagram of the amplifier circuit is shown in figure 2, and the detailed design is shown in figure 3. The signal A from the photomultiplier tube is reduced to a fraction a by the precision potentiometer load resistor. The DC part of the signal is filtered out, and the AC part is amplified by a factor X and put on a pedestal p in the first stage of amplification. The amplifier output is clipped by an amount E_R in order to accentuate the fluctuations of the pulse heights, and to cut the pulse heights below the maximum allowable input signal that the next stage of amplification could tolerate without distortion. In the second stage of amplification, the clipped signal is amplified by a factor Y. The signal from the second stage of amplification is fed to a cathode follower. The cathode-follower output is passed through a capacitor to remove its DC pedestal and is clamped to ground potential. A diode demodulator produces a signal which is a measure of the fluctuations of the water-film thickness. The demodulator circuit is provided with a limiter to protect the measuring instruments against being

overdriven. If there were indications that the limiter was conducting, the input signal was decreased by adjusting the potentiometer. The signal was recorded either on a Honeywell Model 906 Viscicorder or on a General Electric CE Photoelectric Recorder. The Viscicorder had a wide frequency response (flat over a 0–270 c/s range) and was used to record fluctuations in the height. The General Electric recorder was used to record average heights. A Flow Corporation Model TBM r.m.s.-voltmeter was used to measure the power of the AC portion of the signal. A Krohn–Hite Model 330-A ultra-low-frequency band-pass filter was used in the spectral analysis of the AC signal. It has a range of 0·02–2000 c/s.

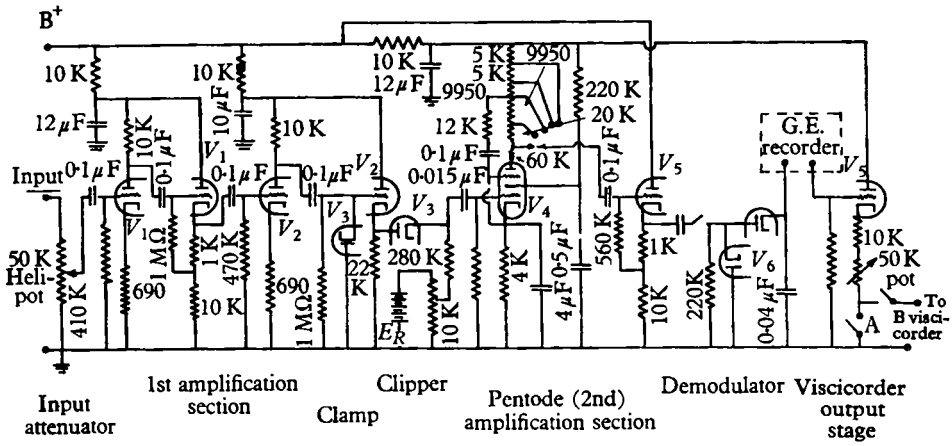

FIGURE 3. Amplifier circuit diagram.

Tubes: V_1, 6SN7; V_2, 6SN7; V_3, 6H6; V_4, 6SJ7; V_5, 6SN7; V_6, 6H6.

The battery supplies were maintained at constant voltages during all runs. The relation between the signal coming from the demodulator and the signal coming from the photomultiplier tube could be varied by changing the potentiometer setting a and the clipping level. The equation describing this relation is

$$R = YXaA + Yp - YE_R. \tag{4.1}$$

The constants Y, X, and p were evaluated by sending a 2 kc/s square wave of known amplitude through the circuit. The circuit was found to behave linearly except at very small attenuator setting a, or at very large clipping levels. The equipment was operated only in the region of linearity.

Equation (4.1) was used to calculate the photomultiplier output A for a given value of the signal R, and for given circuit settings. Since A was directly proportional to the intensity of the light I impinging on the photomultiplier tube, we could write

$$A = k_1 I. \tag{4.2}$$

The intensity I can be related to liquid height h by Lambert's law (Prutton & Maron 1944)

$$I = I_0 e^{-k_2 h}, \tag{4.3}$$

where I_0 is the intensity of the light signal without any liquid in the path and k_2 is a constant which depends on the concentration of methylene-blue dye in the water. Making use of (4.2) and (4.3), we get

$$\frac{I}{I_0} = \frac{A}{A_0} = e^{-k_2 h}. \tag{4.4}$$

The constant k_2 in the above equation was measured for various dye concentrations in the specially constructed cell shown in figure 4. The cell was machined out of Plexiglass, and the flat surfaces were highly polished to remove any scratches. A number of spacers of uniform and known thickness were inserted

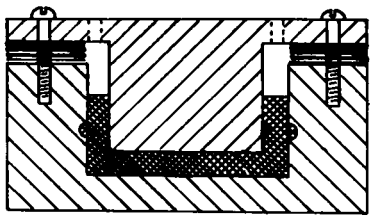

FIGURE 4. Calibration cell (not to scale).

between the bottom and the top part of the cell to vary the liquid-layer thickness in the gap. The effect of the liquid-film thickness on the light transmission for various concentrations of dye in deionized water was measured using the calibrating cell in place of the disk at the bottom of the channel at the test section. The zero level of the photomultiplier output A_0 was measured by removing the cell from the light path. The zero level was inclined to vary, so that during operation it was measured at frequent intervals. Likewise, during extended periods of operation, the effective dye concentration in the test solution varied. Therefore, the effective concentration of dye in the test solution was measured before and after each run.

When power spectral measurements were made, the power passing through the filter for a particular setting of the upper f_2 and the lower f_1 cut-off frequencies was measured with the random-signal voltmeter.

5. Accuracy of height measurements

The chief sources of error in the measurements of the film height were the reflexion and the refraction of light rays at the air–liquid interface. The percentage of the light reflected from the interface of two transparent media depends on the angle of incidence and the refractive index between the media. The percentage of 589 mμ wavelength light reflected from an air–water interface remains constant at about 2 % for low angles of incidence. For light passing from water to air, a significant increase in the amount reflected occurs at angles of incidence larger than about 30°. For light passing from air to water a marked increase occurs at angles of incidence of about 45°. Therefore, height measurements were made using the second mode of operation. However, this choice had the disadvantage that light beams refracted at the surface had a path of travel through the liquid whose length might depend on the angle of inclination of the interface.

This error was calculated to be less than 1 % of the film thickness at angles of incidence less than 30°, and approximately 2 % at an angle of incidence of 40°. These considerations indicate that the method is limited to interfacial slopes of less than about 40°. Of course, the limitations would be more severe for waves whose heights are a very small percentage of the average film height. All of the data reported in this paper, with the exception of the roll wave data, were taken on systems for which the slope of the interface was 40° or less.

Some runs were conducted with no dye in the liquid film. The fluctuation of the signal coming from the height measuring equipment was significant (about 6·3 % fluctuations) only when roll waves were present. These runs indicated that reflexion of light from the interface was not affecting the data appreciably, and that the diffuser plate was operating satisfactorily.

No method was available for comparing directly the photometric wave-height measurements with an independent set of measurements. The depth of the liquid film at the wave crests was estimated with a pointer that could be moved in a direction perpendicular to the channel bottom. The point of contact was determined visually. A reasonable comparison was obtained between these measurements and the sum of the average height and the root-mean-square wave height obtained photometrically.

6. Treatment of data

Average film heights were calculated from the photomultiplier output by (4.4). A fluctuation δh in the film height from the average height is related to a corresponding fluctuation in the photomultiplier output as follows:

$$\delta h = \frac{1}{k_2} \ln\left(\frac{\bar{A}+\delta A}{\bar{A}}\right). \tag{6.1}$$

It should be noted that measurements of fluctuating heights do not depend on the transmission A_0 in the absence of a film. If the fluctuations are small compared with the average amount of light transmitted $\bar{A}$, the following approximation can be used for the wave height:

$$\delta h = \frac{\delta A}{2{\cdot}303\bar{A}k_2}. \tag{6.2}$$

The error due to this approximation in all the data taken was less than one part in 500.

The transfer function $Y(f; f_1; f_2)$ of the band-pass filter was given by the manufacturer as

$$Y(f; f_1; f_2) = \frac{(f/f_1)^4}{[1+2jB(f/f_1)-(f/f_1)^2]^2[1+2jB(f/f_2)-(f/f_2)^2]^2}, \tag{6.3}$$

where B is the peaking factor, equal to 0·6. The frequency spectrum of the waves is related to power from the band-pass filter through the equation

$$\text{Mean power} = \int_0^\infty |Y(f; f_1; f_2)|^2 w(f)\, df. \tag{6.4}$$

A power transfer function can be defined as

$$H(f; f_1; f_2) = |Y(f; f_1; f_2)|^2. \tag{6.5}$$

If the equivalent width of the band-pass window is narrow enough so that the spectral density within the window can be considered as constant and equal to that at the mid-band frequency $f_M = \sqrt{(f_1 f_2)}$, then

$$\text{Mean power} = Kw(f_M), \tag{6.6}$$

$$K = \int_0^\infty H(f; f_1; f_2)\, df. \tag{6.7}$$

The parameter K varies with f_1 and f_2. The spectral density $w(f_M)$ calculated from (6.7) is approximate in that it is based on the assumption of constant power spectrum within the window width. This assumption becomes less objectionable for narrow pass-bands and for spectra varying slowly with frequency. The narrowest pass-band for the filter without undue attenuation is obtained by setting the lower and the upper cut-off frequencies equal. This setting was used in all the measurements reported. The stability of the output signal at this narrowest window setting was not a serious problem because of the large time constant (16 sec) of the random-signal voltmeter used to measure the power.

The assumption of a constant spectral density within the window was checked by comparing the measured total power in the 0·2–60 c/s range with the area under the frequency spectrum curve over the same frequency range. The integral of the frequency spectrum curve yielded 0–10 % lower values. A wider spectral window in which the upper and the lower cut-off frequencies were separated by a factor of 1·75 showed much poorer agreement between the directly measured power and that calculated from the frequency spectrum.

An attempt was made in run *G*, where a 10 % error was noted in power calculated from the spectrum, to obtain a second approximation for the frequency spectrum by applying a linear correction based on the slope of the first approximation to the spectral density curve. The correction has the tendency to lower the spectral-density function in the region of positive slope, and increase it in the high-frequency end of negative slope. The total power of 370×10^{-6} in.^{2} obtained by integrating the corrected frequency spectrum is to be compared with a value of 372×10^{-6} in.^{2} obtained by direct measurement. However, none of the frequency-spectrum results reported in this paper were corrected by this technique.

7. Results

The same type of interfacial structures that were observed by Hanratty & Engen (1957) and by Hershman (1960) with a highly disturbed entry were observed using the specially designed liquid entry described in this paper. The transition to roll waves appeared to be independent of the entry design. However, transition from a smooth surface to one with two-dimensional waves occurred at somewhat higher gas rates with the undisturbed entry. A Visicorder record of the surface structure when three-dimensional waves are present was shown in a previous paper (Lilleleht & Hanratty 1960) for a single flow condition.

Twice the root-mean-square of the fluctuating liquid height, $2\Delta(h')$, is a measure of the wave heights. Figure 5 presents measured values of $\Delta(h')$ as a

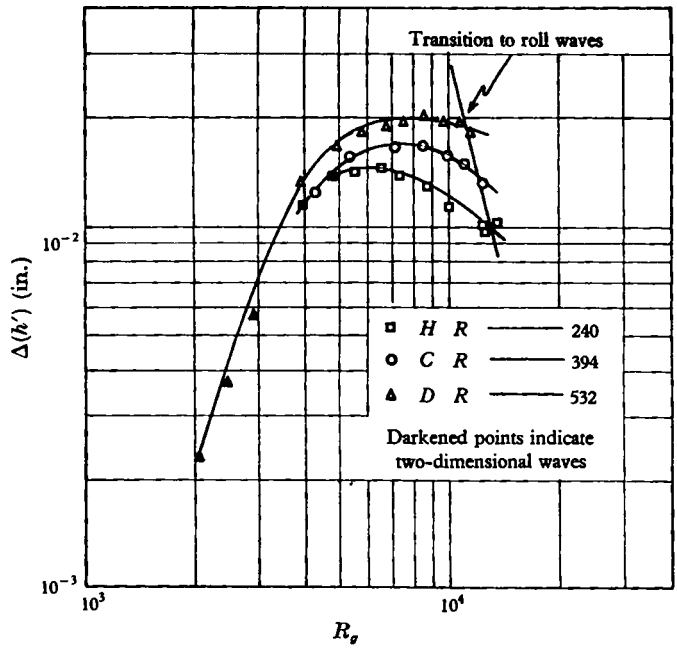

FIGURE 5. Measurements of the root-mean-squared surface displacement.

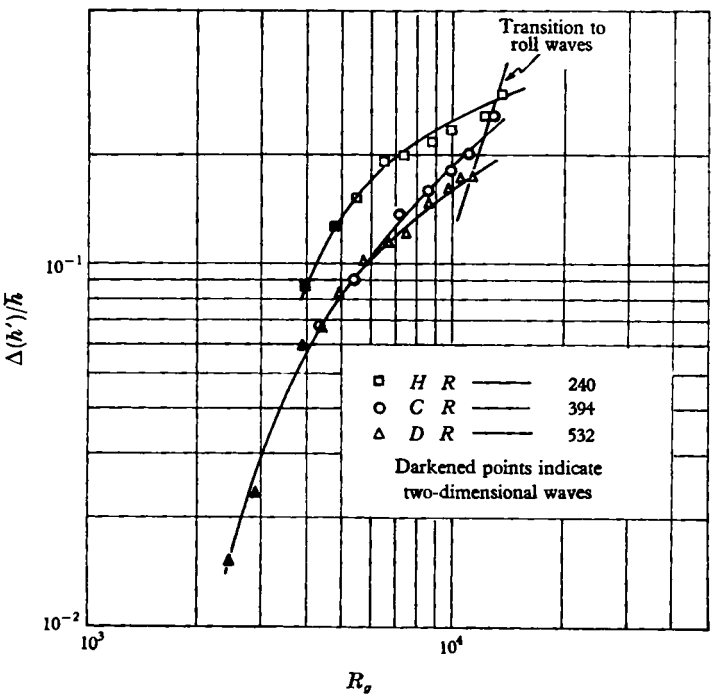

FIGURE 6. Measurements of the root-mean-squared surface displacement, plotted as $\Delta(h')/\bar{h}$.

function of the gas Reynolds number R_g with liquid Reynolds number R as a parameter. The Reynolds numbers are defined in terms of the time-average thicknesses and the mixed average velocities of the air and water layers. The wave height in the region of two-dimensional waves increases markedly with increasing gas Reynolds number. However, in the region of three-dimensional waves, the wave height does not change as rapidly with increasing gas Reynolds number. Measurements of $\Delta(h')/\bar{h}$ are presented in figure 6. For fixed rate of liquid flow (fixed R), the average liquid height $\bar{h}$ decreases with increasing gas

Run	$\bar{h}$ (in.)	$\Delta(h')$ (in.)	R	R_g	u^* (ft./sec)
A†	0·1110	0·0109	239	4,700	0·714
B	0·0743	0·0111	227	8,420	1·285
C	0·1886	0·0126	394	4,350	0·709
D	0·200	0·0166	532	4,930	0·889
E	0·1608	0·0193	532	7,420	1·313
F	0·1129	0·0194	532	10,560	1·820
G	0·1344	0·0193	581	7,300	1·329
H	0·0378	0·0096	240	12,280	1·866

† Two-dimensional waves. All the other runs had a three-dimensional wave structure.

TABLE 1. Run conditions.

Reynolds number R_g, and, therefore, the quantity $\Delta(h')/\bar{h}$ increases with increasing gas Reynolds number. It is to be noted that at high R_g the wave heights approach the magnitude of the average liquid height. Velocity profiles were measured for a number of runs, and friction velocities were calculated. These calculated friction velocities, presented in table 1, were used to correlate measurements of $\Delta(h')$ as shown in figure 7. Spectral measurements are shown in figure 8 for some of the runs summarized in table 1. At small frequencies the spectral function is dependent on the height of the liquid film. However, the high-frequency end of the spectrum for the three-dimensional waves appears to be independent of liquid height since all of the spectral measurements appear to come into a single envelope. A line of slope such that w varies as f^{-5} is shown for reference purposes. Although the high-frequency end of the envelope appears to be described approximately by such a relation, insufficient data have been obtained to say whether any appreciable portion of the envelope obeys this relation and, therefore, is independent of u^*. In run F, a sharp maximum was indicated by the data as at a value of fu^*/g of about 0·035 (0·6 c/s). This run was carried out just below the gas velocity at which roll waves were observed visually. It is possible that this maximum could be due to incipient roll waves. These data have not been presented since it is intended to check them more thoroughly before publication. Values of $(fu^*/g)_{\max}$ and $(wg^3/u^{*5})_{\max}$ are presented as functions of gh/u^{*2} in table 2. The data for $(fu^*/g)_{\max}$ may be represented by the equation

$$(fu^*/g)_{\max} = 0{\cdot}207(g\bar{h}/u^{*2})^{-\frac{1}{2}}. \tag{7.1}$$

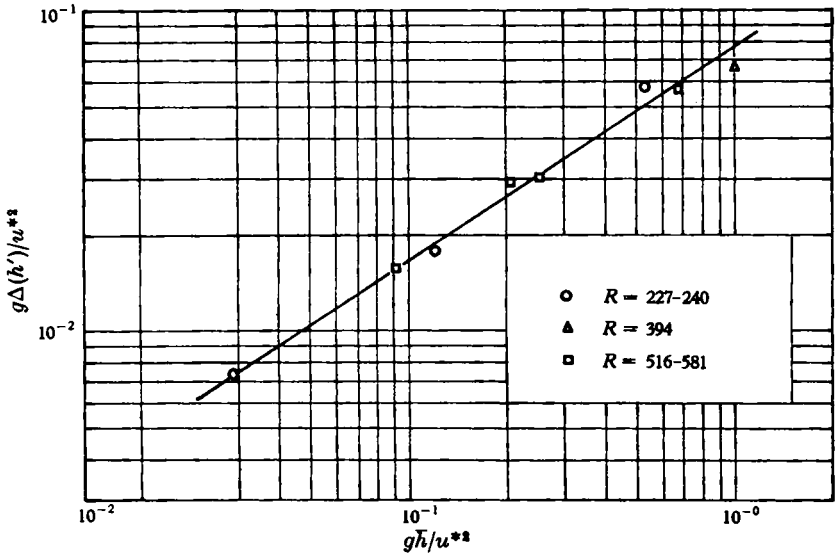

FIGURE 7. Correlation of interfacial displacement measurements.

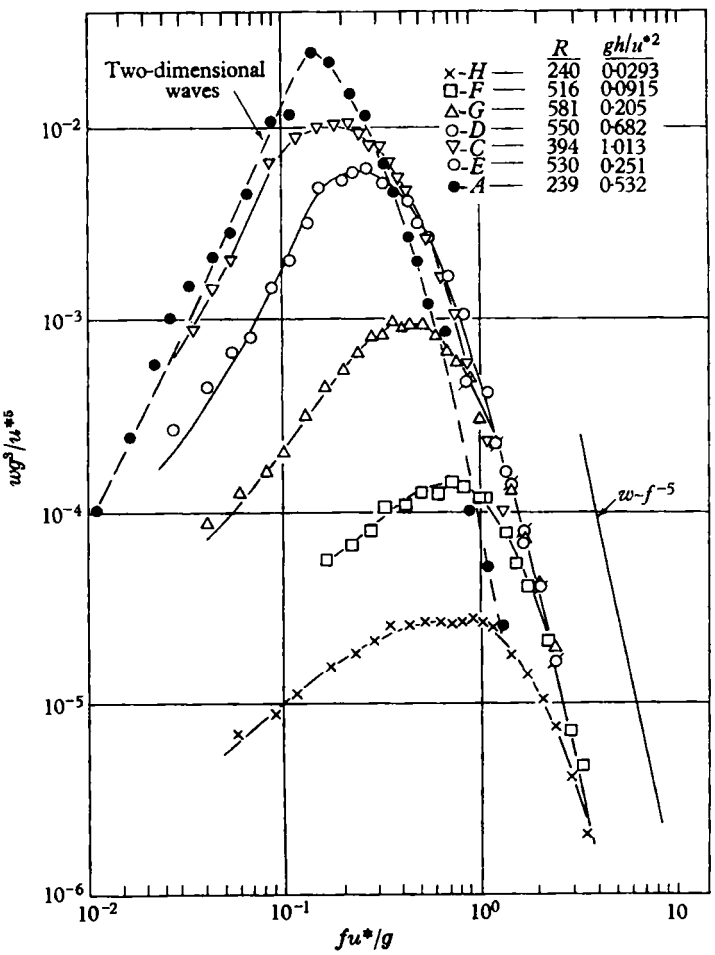

FIGURE 8. Frequency spectra.

This equation indicates that for waves which are affected by the liquid depth, the value of f_{max} is independent of u^* and can be represented by the relation

$$f_{max} = 0{\cdot}207\sqrt{(g/\bar{h})}. \tag{7.2}$$

If the definition of a wave cycle given by Pierson is used (cf. § 2), then $\frac{1}{2}N(\bar{h})$ is the number of waves per second. Values of this parameter measured from Viscicorder wave records are compared with the values of frequency at the

Run	$\frac{g\bar{h}}{u^{*2}}$	$\left(\frac{fu^*}{g}\right)_{max}$	$\left(\frac{wg^3}{u^{*5}}\right)_{max} \times 10^5$	f_{max} (sec^{-1})	$\frac{1}{2}N(\bar{h})$ (sec^{-1})
H	0·0293	0·8	2·7	14	—
F	0·0915	0·7	14	12	26·4
B	0·120	0·52	44	13	—
G	0·205	0·46	95	11	21·2
E	0·251	0·40	120	9·7	22·2
A†	0·532	0·14	2500	6·4	—
D	0·682	0·25	600	9·2	21·9
C	1·013	0·18	1020	8·0	—

† Two-dimensional waves.

TABLE 2. Maxima from the spectral density data.

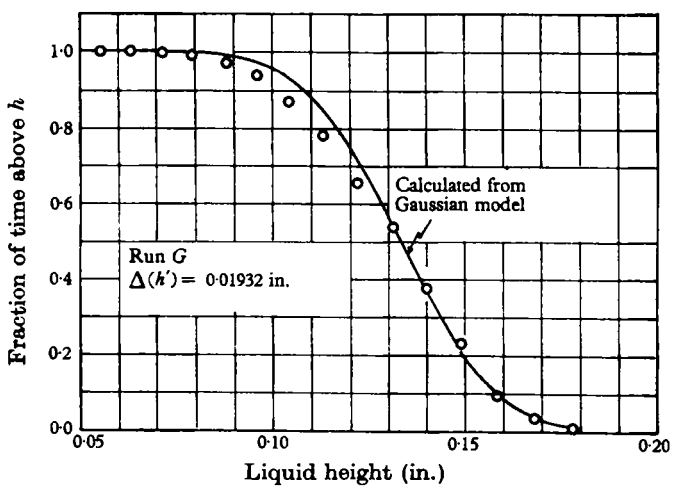

FIGURE 9. Comparison of the wave record with the Gaussian model.

maxima of the spectral density in table 2. It is noted that the maxima are about one half the number of waves per second. As can be seen from figures 7 and 8 and table 2, the measurements of $\Delta(h')$ and of $w(f)$ for three-dimensional waves are correlated quite well by dimensionless groups obtained on neglecting the direct effect of liquid density and viscosity and of interfacial tension. The agreement does not mean that these parameters are not important. The range of physical variables investigated was not sufficient to define the respective roles of fluid properties.

A very long Viscicorder record was analysed for run G to examine the applicability of Gaussian model to the three-dimensional waves observed. Data on

the fraction of the time the fluid is below a given height are presented in figure 9. The curve was calculated from (2.5) by use of the value of $\Delta(h')$ measured with the r.m.s.-voltmeter. In figure 10, measured values of $N(h)/N(\bar{h})$ are compared with those calculated from (2.12). Figure 11 compares the fraction of the crests above a certain value of h, or the fraction of the troughs below h, with curves

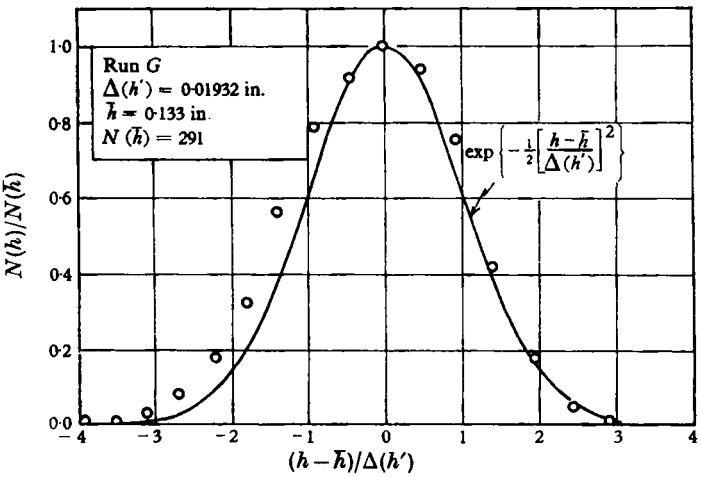

FIGURE 10. Comparison of the measured number of crossings with the Gaussian model.

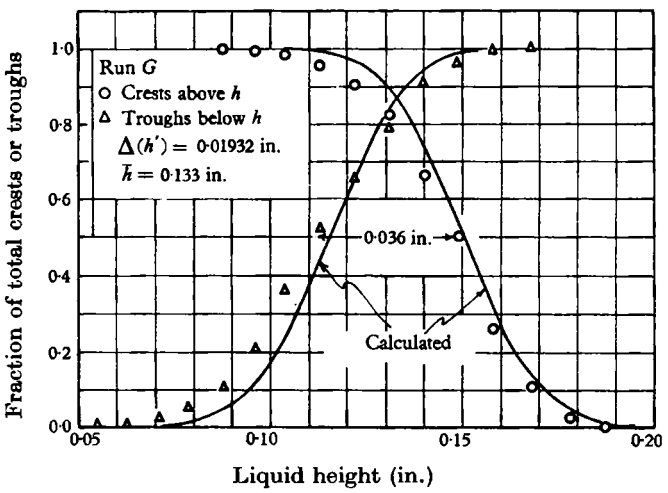

FIGURE 11. Comparison of the measured distribution of crests and troughs with the Gaussian model.

calculated by Rice (1944, 1945) on the basis of the Gaussian model. The measurements in figures 9–11 are approximately described by the Gaussian model. However, the wave structure below $\bar{h}$ appears to be slightly different from the wave structure above $\bar{h}$. It is not certain whether the differences from the Gaussian model are real, or whether they are due to limitations in the experimental technique such as might be caused by refraction effects. This will be explored in future work in this laboratory. The number of zero crossings per

second, $N(\bar{h})$, and the number of maxima per second measured for run G and for three other wave records are presented in table 3. Values of $N(\bar{h})$ calculated from the spectral measurements by use of (2.11) are in very good agreement with

Run	$N(\bar{h})$ (sec^{-1}) Measured	$N(\bar{h})$ (sec^{-1}) Equation (11)	$N(h_m)$ (sec^{-1}) measured
G	42·5	45	33·8
D	43·8	40	59·0
E	44·5	43	68·8
F	52·8	47	82·6

TABLE 3. Number of zero crossings per second and number of maxima per second.

measured values of $N(\bar{h})$. The spectral measurements did not converge to zero rapidly enough at large frequencies to calculate the number of maxima per second from (2.13).

The authors are grateful to the American Oil Company and E. I. duPont deNemours and Company for support.

REFERENCES

CHARVONIA, D. A. 1959 A study of the mean thickness of the liquid film and the characteristics of the interfacial surface in annular two-phase flow in a vertical pipe. *Jet Propulsion Center, Purdue University, Rep.* no. I–59–1.

ELLIS, S. R. M. & GAY, B. 1959 *Trans. Instn Chem. Engrs, Lond.*, **37**, 206.

ELLISON, T. H. 1956 Article in *Surveys in Mechanics*. Cambridge University Press.

ENGEN, J. M. 1956 M.S. Thesis, Dep. Chem. and Chem. Eng., University of Illinois.

GREENBERG, A. B. 1956 Ph.D. Thesis, Purdue University.

HANRATTY, T. J. & ENGEN, J. M. 1957 *J. Amer. Instn Chem. Engrs*, **3**, 299.

HANRATTY, T. J. & HERSHMAN, A. 1960 Initiation of roll waves. Paper presented at Annual Meeting of Amer. Instn Chem. Engrs, Washington, D.C. (December); to be published in *J. Amer. Instn Chem. Engrs*.

HERSHMAN, A. 1960 Ph.D. Thesis, Dep. Chem. and Chem. Eng., University of Illinois.

HICKS, B. L. & WHITTENBURY, C. G. 1956 Wind waves on the water. *Control Systems Lab., University of Illinois, Rep. R*-83.

LILLELEHT, L. U. 1961 Ph.D. Thesis, Dep. Chem. and Chem. Eng., University of Illinois.

LILLELEHT, L. U. & HANRATTY, T. J. 1960 Paper submitted for publication in *J. Amer. Instn Chem. Engrs*.

MCMANUS, H. N. 1959 *Proc. 6th Ann. Conf. on Fluid Mech., University of Texas (September)*.

OOSTERHOUT, K. C. 1958 M.S. Thesis, Dep. Chem. and Chem. Eng., University of Illinois.

PHILLIPS, O. M. 1958 *J. Fluid Mech.* **4**, 426.

PIERSON, W. J. 1955 *Advances in Geophysics*. II. New York: Academic Press.

PRUTTON, C. F. & MARON, S. H. 1944 *Fundamental Principles of Physical Chemistry*, p. 756. London: Macmillan.

VAN ROSSUM, J. J. 1959 *Chem. Engng Sci.* **11**, 35.

PUTZ, R. R. 1954 *Proc. 4th Conf. on Coastal Eng., Coun. of Wave Res., Univ. Calif., Berkeley*, p. 13.

RICE, S. O. 1944 *Bell System Tech. J.* **23**, 282; (1945), *ibid.* **24**, 46.